

Search for Neutral Charmless B Decays at LEP

The L3 Collaboration

Abstract

A search for rare charmless decays of B_d^0 and B_s^0 mesons has been performed in the exclusive channels $B_{d(s)}^0 \rightarrow \eta\eta$, $B_{d(s)}^0 \rightarrow \eta\pi^0$ and $B_{d(s)}^0 \rightarrow \pi^0\pi^0$. The data sample consisted of three million hadronic Z decays collected by the L3 experiment at LEP from 1991 through 1994. No candidate event has been observed and the following upper limits at 90% confidence level on the branching ratios have been set

$$\begin{aligned} \text{Br}(B_d^0 \rightarrow \eta\eta) &< 4.1 \times 10^{-4}, & \text{Br}(B_s^0 \rightarrow \eta\eta) &< 1.5 \times 10^{-3}, \\ \text{Br}(B_d^0 \rightarrow \eta\pi^0) &< 2.5 \times 10^{-4}, & \text{Br}(B_s^0 \rightarrow \eta\pi^0) &< 1.0 \times 10^{-3}, \\ \text{Br}(B_d^0 \rightarrow \pi^0\pi^0) &< 6.0 \times 10^{-5}, & \text{Br}(B_s^0 \rightarrow \pi^0\pi^0) &< 2.1 \times 10^{-4}. \end{aligned}$$

These are the first experimental limits on $B_d^0 \rightarrow \eta\eta$ and on the B_s^0 neutral charmless modes.

Submitted to *Phys. Lett. B*

Introduction

The high statistics data collected by the LEP experiments allow the study of rare B physics processes such as decays with branching ratios in the $10^{-4} - 10^{-5}$ range. This paper describes the search for neutral charmless hadronic decays of B_d^0 and B_s^0 mesons¹⁾ in the neutral exclusive final states:

$$B_d^0 \rightarrow \eta\eta, B_d^0 \rightarrow \eta\pi^0, B_d^0 \rightarrow \pi^0\pi^0, B_s^0 \rightarrow \eta\eta, B_s^0 \rightarrow \eta\pi^0, B_s^0 \rightarrow \pi^0\pi^0.$$

The high resolution of the L3 detector for electromagnetic clusters has been exploited in detecting η 's and π^0 's by means of their decays into pairs of photons as described in Reference [1].

The ALEPH, DELPHI and OPAL experiments at LEP have recently searched for decays of B mesons to charmless charged final states [2], such as:

$$B_d^0 \rightarrow \pi^+\pi^-, B_d^0 \rightarrow K^+\pi^-, B_d^0 \rightarrow K^+K^-, B_s^0 \rightarrow \pi^+\pi^-, B_s^0 \rightarrow K^+\pi^-, B_s^0 \rightarrow K^+K^-,$$

and charge-conjugate modes. The CLEO experiment at CESR, running at the $\Upsilon(4S)$ centre-of-mass energy, has reported on the search for many B_d^0 decay modes [3], observing such charmless decays in the sum of the two modes $B_d^0 \rightarrow \pi^+\pi^-$ and $B_d^0 \rightarrow K^+\pi^-$ [4]. B_s^0 mesons are produced at the centre-of-mass energy $\sqrt{s} \approx m_Z$, while they are not accessible at the $\Upsilon(4S)$ centre-of-mass energy.

In the Standard Model [5], the neutral charmless $B_{d(s)}^0$ decays can occur through a variety of processes such as Cabibbo-suppressed $b \rightarrow u$ transition [6] with a further color suppression with respect to the charged modes [7], or one loop diagrams with a heavy quark and a virtual W^\pm boson [7,8]. Contributions can also arise from electroweak penguins [9]. A set of diagrams, following Reference [8], is shown in Figure 1.

These decay modes can open a window on new physics beyond the Standard Model. In models with two Higgs doublets, additional diagrams with a charged Higgs boson are allowed and can add constructively to the W^\pm boson loop [10]. Minimal Supersymmetric extensions of the Standard Model predict superpartners that could also affect the expected decay rates [11].

The Standard Model theoretical predictions for neutral charmless B_d^0 decays range from 10^{-5} to 10^{-8} [7,12]. No predictions for extensions to the Standard Model exist. The ARGUS experiment at DORIS II has set the 90% confidence level limit $\text{Br}(B_d^0 \rightarrow \eta\pi^0) < 1.8 \times 10^{-3}$ [13]; the limit from CLEO on $B_d^0 \rightarrow \pi^0\pi^0$ is $\text{Br}(B_d^0 \rightarrow \pi^0\pi^0) < 9.1 \times 10^{-6}$, at 90% confidence level [14].

The L3 Detector and Event Simulation

The L3 detector consists of a central tracking chamber, a high resolution crystal electromagnetic calorimeter, a ring of plastic scintillation counters, a uranium and brass hadron calorimeter with proportional wire chamber readout, and an accurate muon chamber system. These detectors are installed in a 12 m diameter magnet which provides a uniform field of 0.5 T along the beam direction. Luminosity is measured with forward BGO arrays on each side of the detector. A detailed description of each detector subsystem and its performance is given in Reference [15].

The subdetectors most relevant for this analysis are the central tracking chamber and the electromagnetic calorimeter. The central tracking chamber is a time expansion chamber (TEC) which consists of two cylindrical layers of 12 and 24 sectors, with a total of 62 wires measuring

¹⁾Throughout this paper charge conjugate mesons \bar{B}_d^0 and \bar{B}_s^0 are also considered.

the R - ϕ coordinate in a plane normal to the beam direction. The z coordinate is measured by a Z -chamber mounted just outside the TEC.

The electromagnetic calorimeter, placed around the TEC, consists of 10734 bismuth germanium oxide (BGO) crystals arranged in two half-barrels with polar angle coverage $42^\circ \leq \theta \leq 138^\circ$ (where θ is defined with respect to the beam axis) and two endcaps covering $10^\circ \leq \theta \leq 38^\circ$ and $142^\circ \leq \theta \leq 170^\circ$. The energy resolution of the BGO calorimeter is $\simeq 5\%$ for photons and electrons with energies around 100 MeV and is less than 2% for energies above 1 GeV. The angular resolution of electromagnetic clusters is better than 0.5° for energies above 1 GeV.

The JETSET 7.4 [16] Monte Carlo, based on the Lund parton shower model, was used to generate a total of 30 000 $Z \rightarrow b\bar{b}$ events, 5 000 events in each of the exclusive decay modes:

$$B_d^0 \rightarrow \eta\eta, B_d^0 \rightarrow \eta\pi^0, B_d^0 \rightarrow \pi^0\pi^0, B_s^0 \rightarrow \eta\eta, B_s^0 \rightarrow \eta\pi^0, B_s^0 \rightarrow \pi^0\pi^0.$$

The b quark on the other side of the event was left free to hadronize and decay. The masses of the generated B_d^0 and B_s^0 mesons were 5.279 GeV and 5.373 GeV respectively. The events were then passed through the full L3 simulation²⁾ which takes into account the effects of energy loss, multiple scattering, interactions and decays in the detector materials. Inefficiencies of the TEC and BGO detectors, obtained from the data, were also simulated. These events, after reconstruction by the same program used for the data, were used to tune the analysis procedure and calculate the efficiency of the rare decays selection criteria.

Background processes were studied using 1.7 million hadronic decays of the Z generated with the JETSET Monte Carlo and passed through the detector simulation and reconstruction chain described above. The Standard Model value $\Gamma_{b\bar{b}}/\Gamma_{\text{had}} = 0.217$ was used for the fraction of Z 's decaying to $b\bar{b}$ with respect to the hadronic decays of the Z . The hadronization of the light quarks was described by the Lund symmetric fragmentation function [16] while the Peterson fragmentation function [19] was used to describe the fragmentation of the c and b quarks. The mean value of the ratio of the energy of the weakly decaying B hadrons to the beam energy used in the generation was $\langle x_E \rangle = 0.703$.

Event Selection

The search for the exclusive neutral decay modes

$$B_d^0 \rightarrow \eta\eta, B_d^0 \rightarrow \eta\pi^0, B_d^0 \rightarrow \pi^0\pi^0, B_s^0 \rightarrow \eta\eta, B_s^0 \rightarrow \eta\pi^0, B_s^0 \rightarrow \pi^0\pi^0.$$

has been performed in 3 088 053 hadronic decays of the Z collected in the years from 1991 through 1994, detecting the η 's and π^0 's through their decay into photons.

Since the hard fragmentation of the b quark gives on average 70% of the beam energy to the B_d^0 or B_s^0 meson, the η/π^0 are likely to have high momentum and the two photons can have a small opening angle. Thus the light mesons can give a single energy cluster in the electromagnetic calorimeter. The analysis was performed in four different final state configurations, which gave the best acceptance and background rejection capability:

²⁾The L3 simulation program is based on the GEANT package [17] with the GHEISHA [18] program for the simulation of hadronic interactions.

- $B_{d(s)}^0 \rightarrow \eta\eta$:
 - four detected photons in the final state,
 - one η giving two detected photons and the other detected as a single cluster,
- $B_{d(s)}^0 \rightarrow \eta\pi^0$:
 - the η detected as two photons and the π^0 as a single cluster,
- $B_{d(s)}^0 \rightarrow \pi^0\pi^0$:
 - both π^0 's detected as single clusters in the final state.

Two classes of variables are relevant for this analysis: the first class allows the identification of photons and single electromagnetic clusters, studying both their purity and kinematics; the second class comprises the description of the global kinematics of the $B_{d(s)}^0$ meson candidate. The background in the former selection consists of charged tracks with energy deposition in the BGO calorimeter, while in the latter, random combinations of electromagnetic clusters have to be rejected. The photons were selected from the full BGO angular coverage with lateral shower shapes consistent with electromagnetic energy depositions, as measured by an estimator, χ_{em}^2 . A cut on the opening angle between the photon candidate and the closest track in the TEC (θ_{3D}) was also used. A minimum energy and a minimum number of crystals were also imposed. Similar criteria were used for the selection of the single clusters from neutral high energy mesons; these clusters are expected to have relatively high energies since the opening angle between the two photons is quite small. Cuts on several global kinematic variables give a powerful rejection of the background:

- The opening angle (θ_{mesons}) of the two light mesons (Figure 2a) is expected to be small, while for random combinations it is peaked toward large angles.
- The hard fragmentation of the b quark gives high energy to the $B_{d(s)}^0$ meson candidate (Figure 2b), whereas background tends to be at low energies.
- The cosine of the angle between the direction of one decay product in the $B_{d(s)}^0$ candidate rest frame and the $B_{d(s)}^0$ candidate flight direction ($\cos\theta^*$) is peaked for the background, while it is expected to be more isotropic for the signal.
- In decay modes where an η is detected as a photon pair, a cut on the invariant mass $M_{\gamma\gamma}$ of these photons can be applied. A flat invariant mass spectrum is expected for random combinations (Figure 2c).
- A constrained fit to the $B_{d(s)}^0$ mass, taking into account the BGO energy and angular resolutions, has been performed for the $B_{d(s)}^0 \rightarrow \pi^0\pi^0$ search. The χ^2 of this fit shows high values for background and low ones for signal (Figure 2d). A cut at the value of 1.6 has been chosen.

These cuts were optimized for the B_d^0 exclusive modes. First a preselection, based on minimal requirements for photons, clusters and B_d^0 candidates was applied; then the distributions of selection variables were examined for Monte Carlo simulations of the B_d^0 and background samples to determine a loose set of cuts. Distributions of the variables for the data were also

compared in order to check that the Monte Carlo described the data well. Satisfactory agreement was found, as shown in Figure 2. The loose cuts were applied to all the variables but one. The distribution of this variable was then studied for data, signal Monte Carlo and background Monte Carlo. Using the Monte Carlo samples a final cut was chosen in order to reject as much background as possible while keeping reasonable efficiency. All the cuts were chosen by repeating this last step for each variable. The same cuts as for the B_d^0 modes have also been applied for the B_s^0 analyses. The final sets of cuts chosen for all final state configurations are reported in Table 1.

	Cut	$B_{d(s)}^0 \rightarrow \eta\eta$ (I)	$B_{d(s)}^0 \rightarrow \eta\eta$ (II)	$B_{d(s)}^0 \rightarrow \eta\pi^0$	$B_{d(s)}^0 \rightarrow \pi^0\pi^0$
Kinematics	$M_{\gamma\gamma}$ (GeV)	0.51–0.58	0.530–0.564	0.530–0.564	-
	$\cos \theta^*$	0.7	0.775	0.75	0.6
	θ_{mesons}	28°	25°	26°	23°
	Total energy	17.0	27.5	25.0	22.0
Photons	Energy (GeV)	0.3	0.5	1.0	-
	χ_{em}^2	10.0	8.0	8.0	-
	θ_{3D} (mrad)	30.0	50.0	50.0	-
Cluster	Energy (GeV)	-	10.0	13.0	6.0
	χ_{em}^2	-	-	8.0	30.0
	θ_{3D} (mrad)	-	50.0	50.0	40.0
2 nd cluster	Energy (GeV)	-	-	-	14.0
	χ_{em}^2	-	-	-	5.0
	θ_{3D} (mrad)	-	-	-	40.0

Table 1: Final cuts for all the B_d^0 and B_s^0 decay modes. The (I) and (II) modes refer to the search for a four photon final state, or one with a photon pair for one η and a single cluster for the other one, respectively. “Kinematics” refers to global kinematic variables of the $B_{d(s)}^0$ candidate, “Photons”, “Cluster” and “2nd cluster” to the cuts on purity of photons, single cluster or most energetic π^0 single cluster, if any.

The energies and the angles of photons from η decay, when detected, have been rescaled in order to minimize the χ^2 of a constrained fit to the η mass that takes into account the energy and angular resolutions of the BGO.

The invariant mass of all the photons and/or clusters of the $B_{d(s)}^0$ candidates, was calculated for all the decay modes. The distribution of this invariant mass for events surviving the cuts in the signal Monte Carlo was fit with a Gaussian of width σ . Events in a $\pm 2\sigma$ window around the fit mass of the $B_{d(s)}^0$ meson were then counted in the signal Monte Carlo and in the data in order to calculate, respectively, the efficiency and the number of $B_{d(s)}^0$ candidates.

Results

The invariant mass spectra for the data and the Gaussians fit to the B_d^0 and B_s^0 Monte Carlo samples after the application of the final cuts are shown in Figure 3.

The efficiencies are given in Table 2 together with their statistical and systematic errors; the systematic errors on efficiencies have been estimated by analyzing events generated with

a harder or softer fragmentation function, *i.e.* with $\langle x_E \rangle = 0.720$ or $\langle x_E \rangle = 0.680$. Other systematic effects are estimated to be small.

Since no candidate event has been found in data for any of the eight final configurations, upper limits at 90% confidence level have been set using the following numerical values: $N_{\text{Had}} = 3\,088\,053$ as the number of Z bosons decaying to hadrons, $\Gamma_{b\bar{b}}/\Gamma_{\text{had}} = 0.222 \pm 0.003(\text{stat.}) \pm 0.007(\text{syst.})$ as the partial width of Z decays into b quark with respect to the hadronic decays [20], $f(b \rightarrow B_d^0) = 39.5 \pm 4.0\%$ and $f(b \rightarrow B_s^0) = 12.0 \pm 3.0\%$ as the fractions of $B_{d(s)}^0$ produced in the fragmentation of b quarks at LEP, in agreement with the available measurements [21], $\text{Br}(\eta \rightarrow \gamma\gamma) = 38.8\%$ and $\text{Br}(\pi^0 \rightarrow \gamma\gamma) = 98.8\%$ [22]. The errors on these numbers and on the efficiencies were taken into account by folding their Gaussian distribution with the Poisson distribution describing the number of expected events.

In the analysis of the $B_{d(s)}^0 \rightarrow \pi^0\pi^0$ the branching ratio of the decay $B_{d(s)}^0 \rightarrow \gamma\gamma$ is assumed to be negligible.

In Table 2 the σ 's of the Gaussian fits to the signal Monte Carlo, the efficiencies and the upper limits set with the procedure described above are reported, for all the considered decay modes.

Process	Resolution	Efficiency	Upper limit 90% C.L.
$B_d^0 \rightarrow \eta\eta$ (I)	107 ± 10 MeV	$2.5 \pm 0.2_{-0.2}^{+0.2}\%$	
$B_d^0 \rightarrow \eta\eta$ (II)	146 ± 11 MeV	$4.6 \pm 0.3_{-0.2}^{+0.02}\%$	
$B_d^0 \rightarrow \eta\eta$			$< 4.1 \times 10^{-4}$
$B_d^0 \rightarrow \eta\pi^0$	79 ± 5 MeV	$4.5 \pm 0.3_{-0.03}^{+0.05}\%$	$< 2.5 \times 10^{-4}$
$B_d^0 \rightarrow \pi^0\pi^0$	97 ± 4 MeV	$7.6 \pm 0.4_{-0.5}^{+0.2}\%$	$< 6.0 \times 10^{-5}$
$B_s^0 \rightarrow \eta\eta$ (I)	101 ± 10 MeV	$2.4 \pm 0.2_{-0.2}^{+0.2}\%$	
$B_s^0 \rightarrow \eta\eta$ (II)	129 ± 8 MeV	$4.8 \pm 0.3_{-0.3}^{+0.2}\%$	
$B_s^0 \rightarrow \eta\eta$			$< 1.5 \times 10^{-3}$
$B_s^0 \rightarrow \eta\pi^0$	81 ± 1 MeV	$4.3 \pm 0.3_{-0.1}^{+0.02}\%$	$< 1.0 \times 10^{-3}$
$B_s^0 \rightarrow \pi^0\pi^0$	99 ± 4 MeV	$8.3 \pm 0.4_{-0.7}^{+0.4}\%$	$< 2.1 \times 10^{-4}$

Table 2: Resolutions (σ of a Gaussian fit to the signal Monte Carlo invariant mass distribution), efficiencies and experimental limits for B_d^0 and B_s^0 branching ratios. The (I) and (II) modes refer respectively to the search for a four photon final state or one with a photon pair for one η and a single cluster for the other one. The first error on the efficiencies is statistical, the second systematic.

Conclusions

A search for rare charmless decays of B_d^0 and B_s^0 mesons has been performed in the exclusive modes $B_{d(s)}^0 \rightarrow \eta\eta$, $B_{d(s)}^0 \rightarrow \eta\pi^0$ and $B_{d(s)}^0 \rightarrow \pi^0\pi^0$, detecting η 's and π^0 's by means of their decays into photons. No candidate events have been found and upper limits on the branching ratios at 90% confidence level were set as:

$$\begin{aligned} \text{Br}(B_d^0 \rightarrow \eta\eta) &< 4.1 \times 10^{-4}, \quad \text{Br}(B_s^0 \rightarrow \eta\eta) < 1.5 \times 10^{-3}, \\ \text{Br}(B_d^0 \rightarrow \eta\pi^0) &< 2.5 \times 10^{-4}, \quad \text{Br}(B_s^0 \rightarrow \eta\pi^0) < 1.0 \times 10^{-3}, \\ \text{Br}(B_d^0 \rightarrow \pi^0\pi^0) &< 6.0 \times 10^{-5}, \quad \text{Br}(B_s^0 \rightarrow \pi^0\pi^0) < 2.1 \times 10^{-4}. \end{aligned}$$

The $B_d^0 \rightarrow \eta\eta$ and B_s^0 limits are the first ones set, while the $B_d^0 \rightarrow \eta\pi^0$ limit improves the existing one [13] by almost an order of magnitude.

Acknowledgments

We wish to express our gratitude to the CERN accelerator divisions for the excellent performance of the LEP machine. We acknowledge the contributions of all the engineers and technicians who have participated in the construction and maintenance of this experiment. Those of us who are not from member states thank CERN for its hospitality and help.

The L3 Collaboration:

M. Acciarri,²⁷ A. Adam,⁴⁶ O. Adriani,¹⁷ M. Aguilar-Benitez,²⁶ S. Ahlen,¹¹ B. Alpat,³⁴ J. Alcaraz,²⁶ J. Allaby,¹⁸ A. Aloisio,²⁹ G. Alverson,¹² M. G. Alvigi,²⁹ G. Ambrosi,³⁴ H. Anderhub,⁴⁹ V. P. Andreev,³⁸ T. Angelescu,¹³ D. Antreasyan,⁹ A. Arefev,²⁸ T. Azemoon,³ T. Aziz,¹⁰ P. Bagnaia,^{37,18} L. Baksay,⁴⁴ R. C. Ball,³ S. Banerjee,¹⁰ K. Banicz,⁴⁶ R. Barillere,¹⁸ L. Barone,³⁷ P. Bartalini,³⁴ A. Baschirotto,²⁷ M. Basile,⁹ R. Battiston,³⁴ A. Bay,²³ F. Becattini,¹⁷ U. Becker,¹⁶ F. Behner,⁴⁹ Gy. L. Bencze,¹⁴ J. Berdugo,²⁶ P. Berges,¹⁶ B. Bertucci,¹⁸ B. L. Betev,⁴⁹ M. Biasini,³⁴ A. Biland,⁴⁹ G. M. Bilei,³⁴ R. Bizzarri,³⁷ J. J. Blaising,¹⁸ G. J. Bobbink,² R. Bock,¹ A. Böhm,¹ B. Borgia,³⁷ A. Boucham,⁴ D. Bourilkov,⁴⁹ M. Bourquin,²⁰ D. Boutigny,⁴ E. Brambilla,¹⁶ J. G. Branson,⁴⁰ V. Brigljevic,⁴⁹ I. C. Brock,³⁵ A. Buijs,⁴⁵ A. Bujak,⁴⁶ J. D. Burger,¹⁶ W. J. Burger,²⁰ C. Burgos,²⁶ J. Busenitz,⁴⁴ A. Buytenhuijs,³¹ X. D. Cai,¹⁹ M. Capell,¹⁶ G. Cara Romeo,⁹ M. Caria,³⁴ G. Carlino,²⁹ A. M. Cartacci,¹⁷ J. Casaus,²⁶ G. Castellini,¹⁷ R. Castello,²⁷ F. Cavallari,³⁷ N. Cavallo,²⁹ C. Cecchi,²⁰ M. Cerrada,²⁶ F. Cesaroni,³⁷ M. Chamizo,²⁶ A. Chan,⁵¹ Y. H. Chang,⁵¹ U. K. Chaturvedi,¹⁹ M. Chemarin,²⁵ A. Chen,⁵¹ C. Chen,⁷ G. Chen,⁷ G. M. Chen,⁷ H. F. Chen,²¹ H. S. Chen,⁷ M. Chen,¹⁶ G. Chiefari,²⁹ C. Y. Chien,⁵ M. T. Choi,⁴³ L. Cifarelli,³⁹ F. Cindolo,⁹ C. Civinini,¹⁷ I. Clare,¹⁶ R. Clare,¹⁶ T. E. Coan,²⁴ H. O. Cohn,³² G. Coignet,⁴ A. P. Colijn,² N. Colino,¹⁸ V. Commichau,¹ S. Costantini,³⁷ F. Cotorobai,¹³ B. de la Cruz,²⁶ T. S. Dai,¹⁶ R. D' Alessandro,¹⁷ R. de Asmundis,²⁹ H. De Boeck,³¹ A. Degré,⁴ K. Deiters,⁴⁷ E. Dénes,¹⁴ P. Denes,³⁶ F. DeNotaristefani,³⁷ D. DiBitonto,⁴⁴ M. Diemoz,³⁷ D. van Dierendonck,² F. Di Lodovico,³⁷ C. Dionisi,³⁷ M. Dittmar,⁴⁹ A. Dominguez,⁴⁰ A. Doria,²⁹ I. Dorne,⁴ M. T. Dova,^{19,8} E. Drago,²⁹ D. Duchesneau,¹⁸ P. Duinker,² I. Duran,⁴¹ S. Dutta,¹⁰ S. Easo,³⁴ Yu. Efremenko,³² H. El Mamouni,²⁵ A. Engler,³⁵ F. J. Eppling,¹⁶ F. C. Erné,² J. P. Ernenwein,²⁵ P. Extermann,²⁰ R. Fabbretti,⁴⁷ M. Fabre,³⁷ R. Faccini,³⁷ S. Falciano,³⁷ A. Favara,¹⁷ J. Fay,²⁵ M. Felcini,⁴⁹ T. Ferguson,³⁵ D. Fernandez,²⁶ G. Fernandez,²⁶ F. Ferroni,³⁷ H. Fesefeldt,¹ E. Fiandrin,³⁴ J. H. Field,²⁰ F. Filthaut,³⁵ P. H. Fisher,¹⁶ G. Forconi,¹⁶ L. Fredj,²⁰ K. Freudenreich,⁴⁹ M. Gailoud,²³ Yu. Galaktionov,^{28,16} S. N. Ganguli,¹⁰ P. Garcia-Abia,²⁶ S. S. Gau,¹² S. Gentile,³⁷ J. Gerald,⁵ N. Gheordanescu,¹³ S. Giagu,³⁷ S. Goldfarb,²³ J. Goldstein,¹¹ Z. F. Gong,²¹ E. Gonzalez,²⁶ A. Gougas,⁵ D. Goujon,²⁰ G. Gratta,³³ M. W. Gruenewald,⁸ V. K. Gupta,³⁶ A. Gurtu,¹⁰ H. R. Gustafson,³ L. J. Gutay,⁴⁶ B. Hartmann,¹ A. Hasan,³⁰ J. T. He,⁷ T. Hebbeker,⁸ A. Hervé,¹⁸ K. Hilgers,¹ W. C. van Hoek,³¹ H. Hofer,⁴⁹ H. Hoorani,²⁰ S. R. Hou,⁵¹ G. Hu,¹⁹ M. M. Ilyas,¹⁹ V. Innocent,¹⁸ H. Janssen,⁴ B. N. Jin,⁷ L. W. Jones,³ P. de Jong,¹⁶ I. Josa-Mutuberria,²⁶ A. Kasser,²³ R. A. Khan,¹⁹ Yu. Kamyshev,³² P. Kapinos,⁴⁸ J. S. Kapustinsky,²⁴ Y. Karyotakis,⁴ M. Kaur,^{19,◇} M. N. Kienzle-Focacci,²⁰ D. Kim,⁵ J. K. Kim,⁴³ S. C. Kim,⁴³ Y. G. Kim,⁴³ W. W. Kinnison,²⁴ A. Kirkby,³³ D. Kirkby,³³ J. Kirkby,¹⁸ W. Kittel,³¹ A. Klimentov,^{16,28} A. C. König,³¹ E. Koffeman,¹ O. Kornadt,¹ V. Koutsenko,^{16,28} A. Koulbardi,³⁸ R. W. Kraemer,³⁵ T. Kramer,¹⁶ W. Krenz,¹ H. Kuijten,³¹ A. Kunin,^{16,28} P. Ladron de Guevara,²⁶ G. Landi,¹⁷ C. Lapoint,¹⁶ K. Lassila-Perini,⁴⁹ P. Laurikainen,²² M. Lebeau,¹⁸ A. Lebedev,¹⁶ P. Lebrun,²⁵ P. Lecomte,⁴⁹ P. Lecoq,¹⁸ P. Le Coultre,⁴⁹ J. S. Lee,⁴³ K. Y. Lee,⁴³ C. Leggett,³ J. M. Le Goff,⁸ R. Leiste,⁴⁸ M. Lenti,¹⁷ E. Leonardi,³⁷ P. Levchenko,³⁸ C. Li,²¹ E. Lieb,⁴⁸ W. T. Lin,⁵¹ F. L. Linde,² B. Lindemann,¹ L. Lista,²⁹ Z. A. Liu,⁷ W. Lohmann,⁴⁸ E. Longo,³⁷ W. Lu,³³ Y. S. Lu,⁷ K. Lübelmeyer,¹ C. Luci,³⁷ D. Luckey,¹⁶ L. Ludovici,³⁷ L. Luminari,³⁷ W. Lustermann,⁴⁷ W. G. Ma,²¹ A. Macchiolo,¹⁷ M. Maity,¹⁰ L. Malgeri,³⁷ A. Malinin,²⁸ C. Mañá,²⁶ S. Mangla,¹⁰ M. Maolinbay,⁴⁹ P. Marchesini,⁴⁹ A. Marin,¹¹ J. P. Martin,²⁵ F. Marzano,³⁷ G. G. G. Massaro,² K. Mazumdar,¹⁰ D. McNally,¹⁸ S. Mele,²⁹ L. Merola,²⁹ M. Meschini,¹⁷ W. J. Metzger,³¹ Y. Mi,²³ A. Mihul,¹³ A. J. W. van Mil,³¹ G. Mirabelli,³⁷ J. Mnich,¹⁸ M. Möller,¹ B. Montealeoni,¹⁷ R. Moore,³ R. Morand,⁴ S. Morganti,³⁷ R. Mount,³³ S. Müller,¹ F. Muheim,²⁰ E. Nagy,¹⁴ S. Nahn,¹⁶ M. Napolitano,²⁹ F. Nessi-Tedaldi,⁴⁹ H. Newman,³³ A. Nippe,¹ H. Nowak,⁴⁸ G. Organtini,³⁷ R. Ostonen,²² D. Pandoulas,¹ S. Paoletti,³⁷ P. Paolucci,²⁹ G. Pascale,³⁷ G. Passaleva,¹⁷ S. Patricelli,²⁹ T. Paul,³⁴ M. Pauluzzi,³⁴ C. Paus,¹ F. Pauss,⁴⁹ Y. J. Pei,¹ S. Pensotti,²⁷ D. Perret-Gallix,⁴ S. Petrak,⁸ A. Pevsner,⁵ D. Piccolo,²⁹ M. Pieri,¹⁷ J. C. Pinto,³⁵ P. A. Piroué,³⁶ E. Pistolesi,¹⁷ V. Plyaskin,²⁸ M. Pohl,⁴⁹ V. Pojidaev,^{28,17} H. Postema,¹⁶ N. Produit,²⁰ R. Raghavan,¹⁰ G. Rahal-Callot,⁴⁹ P. G. Rancoita,²⁷ M. Rattaggi,²⁷ G. Raven,⁴⁰ P. Razi,³⁰ K. Read,³² M. Redaelli,²⁷ D. Ren,⁴⁹ M. Rescigno,³⁷ S. Reucroft,¹² A. Ricker,¹ S. Riemann,⁴⁸ B. C. Riemers,⁴⁶ K. Riles,³ O. Rind,³ S. Ro,⁴³ A. Robohm,⁴⁹ J. Rodin,¹⁶ F. J. Rodriguez,²⁶ B. P. Roe,³ M. Röhner,¹ S. Röhner,¹ L. Romero,²⁶ S. Rosier-Lees,⁴ Ph. Rosset,²³ W. van Rossum,⁴⁵ S. Roth,¹ J. A. Rubio,¹⁸ H. Rykaczewski,⁴⁹ J. Salicio,¹⁸ J. M. Salicio,²⁶ E. Sanchez,²⁶ A. Santocchia,³⁴ M. E. Sarakinos,²² S. Sarkar,¹⁰ M. Sassowsky,¹ G. Sauvage,⁴ C. Schäfer,¹ V. Schegelsky,³⁸ D. Schmitz,¹ P. Schmitz,¹ M. Schneegans,⁴ B. Schoeneich,⁴⁸ N. Scholz,⁴⁹ H. Schopper,⁵⁰ D. J. Schotanus,³¹ R. Schulte,¹ K. Schultze,¹ J. Schwenke,¹ G. Schwering,¹ C. Sciacca,²⁹ P. G. Seiler,⁴⁷ J. C. Sens,⁵¹ L. Servoli,³⁴ S. Shevchenko,³³ N. Shivarov,⁴² V. Shoutko,²⁸ J. Shukla,²⁴ E. Shumilov,²⁸ D. Son,⁴³ A. Sopczak,¹⁸ V. Soulimov,²⁹ B. Smith,¹⁶ T. Spickermann,¹ P. Spillantini,¹⁷ M. Steuer,¹⁶ D. P. Stickland,³⁶ F. Sticozzi,¹⁶ H. Stone,³⁶ B. Stoyanov,⁴² K. Strauch,¹⁵ K. Sudhakar,¹⁰ G. Sultanov,¹⁹ L. Z. Sun,²¹ G. F. Susinno,²⁰ H. Suter,⁴⁹ J. D. Swain,¹⁹ X. W. Tang,⁷ L. Tauscher,⁶ L. Taylor,¹² Samuel C. C. Ting,¹⁶ S. M. Ting,¹⁶ O. Toker,³⁴ F. Tonisch,⁴⁸ M. Tonutti,¹ S. C. Tonwar,¹⁰ J. Tóth,¹⁴ A. Tsaregorodtsev,³⁸ G. Tsipolitis,³⁵ C. Tully,³⁶ H. Tuchscherer,⁴⁴ J. Ulbricht,⁴⁹ L. Urbán,¹⁴ U. Uwer,¹ E. Valente,³⁷ R. T. Van de Walle,³¹ I. Vetlitsky,²⁸ G. Viertel,⁴⁹ M. Vivargent,⁴ R. Völkert,⁴⁸ H. Vogel,³⁵ H. Vogt,⁴⁸ I. Vorobiev,²⁸ A. A. Vorobyov,³⁸ An. A. Vorobyov,³⁸ L. Vuilleumier,²³ M. Wadhwa,⁶ W. Wallraff,¹ J. C. Wang,¹⁶ X. L. Wang,²¹ Y. F. Wang,¹⁶ Z. M. Wang,²¹ A. Weber,¹ R. Weill,²³ C. Willmott,²⁶ F. Wittgenstein,¹⁸ S. X. Wu,¹⁹ S. Wynhoff,¹ J. Xu,¹¹ Z. Z. Xu,²¹ B. Z. Yang,²¹ C. G. Yang,⁷ X. Y. Yao,⁷ J. B. Ye,²¹ S. C. Yeh,⁵¹ J. M. You,³⁵ C. Zaccardelli,³³ An. Zalite,³⁸ P. Zemp,⁴⁹ J. Y. Zeng,⁷ Y. Zeng,¹ Z. Zhang,⁷ Z. P. Zhang,²¹ B. Zhou,¹¹ G. J. Zhou,⁷ J. F. Zhou,¹ Y. Zhou,³ G. Y. Zhu,⁷ R. Y. Zhu,³³ A. Zichichi,^{9,18,19} B. C. C. van der Zwaan.²

-
- 1 I. Physikalisches Institut, RWTH, D-52056 Aachen, FRG[§]
 - III. Physikalisches Institut, RWTH, D-52056 Aachen, FRG[§]
 - 2 National Institute for High Energy Physics, NIKHEF, and University of Amsterdam, NL-1009 DB Amsterdam, The Netherlands
 - 3 University of Michigan, Ann Arbor, MI 48109, USA
 - 4 Laboratoire d'Annecy-le-Vieux de Physique des Particules, LAPP, IN2P3-CNRS, BP 110, F-74941 Annecy-le-Vieux CEDEX, France
 - 5 Johns Hopkins University, Baltimore, MD 21218, USA
 - 6 Institute of Physics, University of Basel, CH-4056 Basel, Switzerland
 - 7 Institute of High Energy Physics, IHEP, 100039 Beijing, China
 - 8 Humboldt University, D-10099 Berlin, FRG[§]
 - 9 INFN-Sezione di Bologna, I-40126 Bologna, Italy
 - 10 Tata Institute of Fundamental Research, Bombay 400 005, India
 - 11 Boston University, Boston, MA 02215, USA
 - 12 Northeastern University, Boston, MA 02115, USA
 - 13 Institute of Atomic Physics and University of Bucharest, R-76900 Bucharest, Romania
 - 14 Central Research Institute for Physics of the Hungarian Academy of Sciences, H-1525 Budapest 114, Hungary[‡]
 - 15 Harvard University, Cambridge, MA 02139, USA
 - 16 Massachusetts Institute of Technology, Cambridge, MA 02139, USA
 - 17 INFN Sezione di Firenze and University of Florence, I-50125 Florence, Italy
 - 18 European Laboratory for Particle Physics, CERN, CH-1211 Geneva 23, Switzerland
 - 19 World Laboratory, FBLJA Project, CH-1211 Geneva 23, Switzerland
 - 20 University of Geneva, CH-1211 Geneva 4, Switzerland
 - 21 Chinese University of Science and Technology, USTC, Hefei, Anhui 230 029, China
 - 22 SEFT, Research Institute for High Energy Physics, P.O. Box 9, SF-00014 Helsinki, Finland
 - 23 University of Lausanne, CH-1015 Lausanne, Switzerland
 - 24 Los Alamos National Laboratory, Los Alamos, NM 87544, USA
 - 25 Institut de Physique Nucléaire de Lyon, IN2P3-CNRS, Université Claude Bernard, F-69622 Villeurbanne Cedex, France
 - 26 Centro de Investigaciones Energeticas, Medioambientales y Tecnológicas, CIEMAT, E-28040 Madrid, Spain
 - 27 INFN-Sezione di Milano, I-20133 Milan, Italy
 - 28 Institute of Theoretical and Experimental Physics, ITEP, Moscow, Russia
 - 29 INFN-Sezione di Napoli and University of Naples, I-80125 Naples, Italy
 - 30 Department of Natural Sciences, University of Cyprus, Nicosia, Cyprus
 - 31 University of Nymegen and NIKHEF, NL-6525 ED Nymegen, The Netherlands
 - 32 Oak Ridge National Laboratory, Oak Ridge, TN 37831, USA
 - 33 California Institute of Technology, Pasadena, CA 91125, USA
 - 34 INFN-Sezione di Perugia and Università Degli Studi di Perugia, I-06100 Perugia, Italy
 - 35 Carnegie Mellon University, Pittsburgh, PA 15213, USA
 - 36 Princeton University, Princeton, NJ 08544, USA
 - 37 INFN-Sezione di Roma and University of Rome, "La Sapienza", I-00185 Rome, Italy
 - 38 Nuclear Physics Institute, St. Petersburg, Russia
 - 39 University and INFN, Salerno, I-84100 Salerno, Italy
 - 40 University of California, San Diego, CA 92093, USA
 - 41 Dept. de Física de Partículas Elementales, Univ. de Santiago, E-15706 Santiago de Compostela, Spain
 - 42 Bulgarian Academy of Sciences, Central Laboratory of Mechatronics and Instrumentation, BU-1113 Sofia, Bulgaria
 - 43 Center for High Energy Physics, Korea Advanced Inst. of Sciences and Technology, 305-701 Taejeon, Republic of Korea
 - 44 University of Alabama, Tuscaloosa, AL 35486, USA
 - 45 Utrecht University and NIKHEF, NL-3584 CB Utrecht, The Netherlands
 - 46 Purdue University, West Lafayette, IN 47907, USA
 - 47 Paul Scherrer Institut, PSI, CH-5232 Villigen, Switzerland
 - 48 DESY-Institut für Hochenergiephysik, D-15738 Zeuthen, FRG
 - 49 Eidgenössische Technische Hochschule, ETH Zürich, CH-8093 Zürich, Switzerland
 - 50 University of Hamburg, D-22761 Hamburg, FRG
 - 51 High Energy Physics Group, Taiwan, China
- § Supported by the German Bundesministerium für Bildung, Wissenschaft, Forschung und Technologie
‡ Supported by the Hungarian OTKA fund under contract numbers 2970 and T14459.
b Supported also by the Comisión Interministerial de Ciencia y Tecnología

‡ Also supported by CONICET and Universidad Nacional de La Plata, CC 67, 1900 La Plata, Argentina
◇ Also supported by Panjab University, Chandigarh-160014, India

References

- [1] L3 Collab., M. Acciarri *et al.*, Phys. Lett. **B 328** (1994) 223.
- [2] A. M. Litke, in Proceedings of the XXVII International Conference on High Energy Physics, Glasgow, ed. I. G. Knowles P. J. Bussey, (Institute of Physics Publishing, Bristol and Philadelphia, 1994), p. 1333;
OPAL Collab., R. Akers *et al.*, Phys. Lett. **B337** (1994) 393;
DELPHI Collab., P. Abreu *et al.*, Preprint CERN-PPE/95-91.
- [3] E. H. Thorndike, in Proceedings of the XXVII International Conference on High Energy Physics, Glasgow, ed. I. G. Knowles P. J. Bussey, (Institute of Physics Publishing, Bristol and Philadelphia, 1994), p. 1327.
- [4] CLEO Collab., M. Battle *et al.*, Phys. Rev. Lett. **71** (1993) 3922.
- [5] S.L. Glashow, Nucl. Phys. **22** (1961) 579;
S. Weinberg, Phys. Rev. Lett. **19** (1967) 1264;
A. Salam, in Elementary Particle Theory, ed. N. Svartholm, (Almqvist and Wiksell, Stockholm, 1968), p. 367.
- [6] N. Cabibbo, Phys. Rev. Lett. **10** (1963) 531;
M. Kobayashi, T. Maskawa, Prog. Theo. Phys. **49** (1973) 652.
- [7] L. L. Chau *et al.*, Phys. Rev. **D43** (1991) 2176.
- [8] M. Gronau *et al.*, Preprint TECHNION-PH-95-10;
M. Gronau *et al.*, Preprint TECHNION-PH-94-8.
- [9] M. Gronau *et al.*, Preprint TECHNION-PH-95-11.
- [10] S. L. Glashow, E. E. Jenkins, Phys. Lett. **B196** (1987) 233.
- [11] R. Barbieri, G. F. Giudice, Preprint CERN-TH.6830/93.
- [12] F. Buccella *et al.*, Il Nuovo Cimento **104 A n.9** (1991) 1293;
A. Deandrea *et al.*, Phys. Lett. **B318** (1993) 549.
- [13] ARGUS Collab., H. Albrecht *et al.*, Phys. Lett. **B241** (1990) 278.
- [14] CLEO Collab., D.M. Asner *et al.*, Preprint CLNS 95/1338.
- [15] L3 Collab., B. Adeva *et al.*, Nucl. Inst. Meth. **A 289** (1990) 35;
L3 Collab., O. Adriani *et al.*, Physics Reports **236** (1993) 1.
- [16] T. Sjöstrand, Computer Physics Commun. **82** (1994) 74;
T. Sjöstrand, Preprint CERN-TH.7112/93.
- [17] R. Brun *et al.*, “GEANT 3”, CERN DD/EE/84-1 (Revised), September 1987.
- [18] H.Fesefeldt, Preprint RWTH Aachen PITHA 85/02 (1985).
- [19] C. Peterson *et al.*, Phys. Rev. **D 27** (1983) 105.

- [20] L3 Collab., O. Adriani *et al.*, *Phys. Lett.* **B 307** (1993) 237.
- [21] OPAL Collab., R. Akers *et al.*, *Z. Phys.* **C 66** (1995) 555;
OPAL Collab., R. Akers *et al.*, *Z. Phys.* **C 67** (1995) 57;
ALEPH Collab., D. Buskulic *et al.*, Preprint CERN-PPE/95-092;
ALEPH Collab., D. Buskulic *et al.*, Preprint CERN-PPE/95-094.
- [22] Particle Data Group, *Phys. Rev.* **D 50** (1994) 1173.

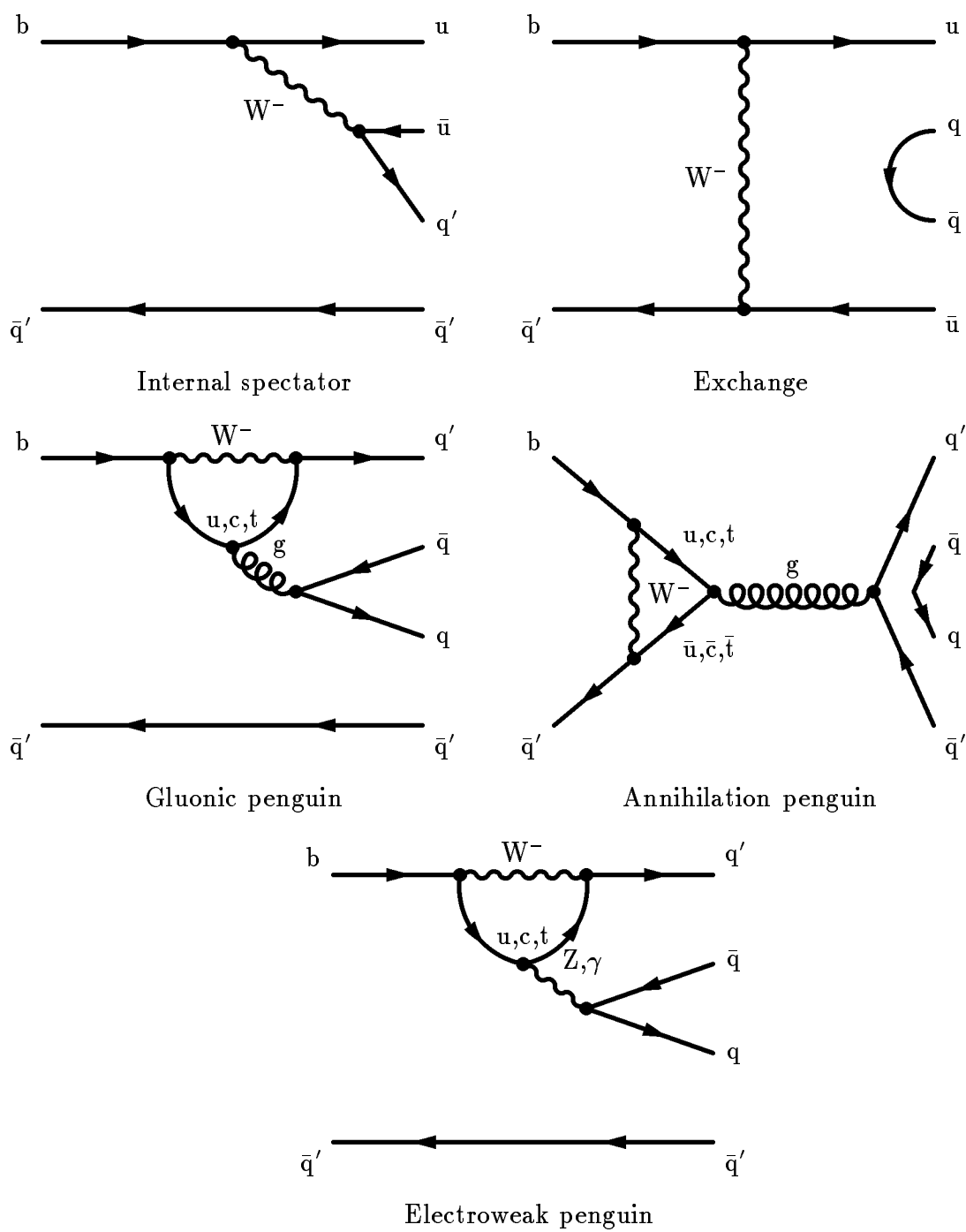


Figure 1: Diagrams leading to $B_{d(s)}^0 \rightarrow \eta\eta$, $B_{d(s)}^0 \rightarrow \eta\pi^0$ and $B_{d(s)}^0 \rightarrow \pi^0\pi^0$ decays. q stands for a u , d or s quark while q' is either a d or an s quark.

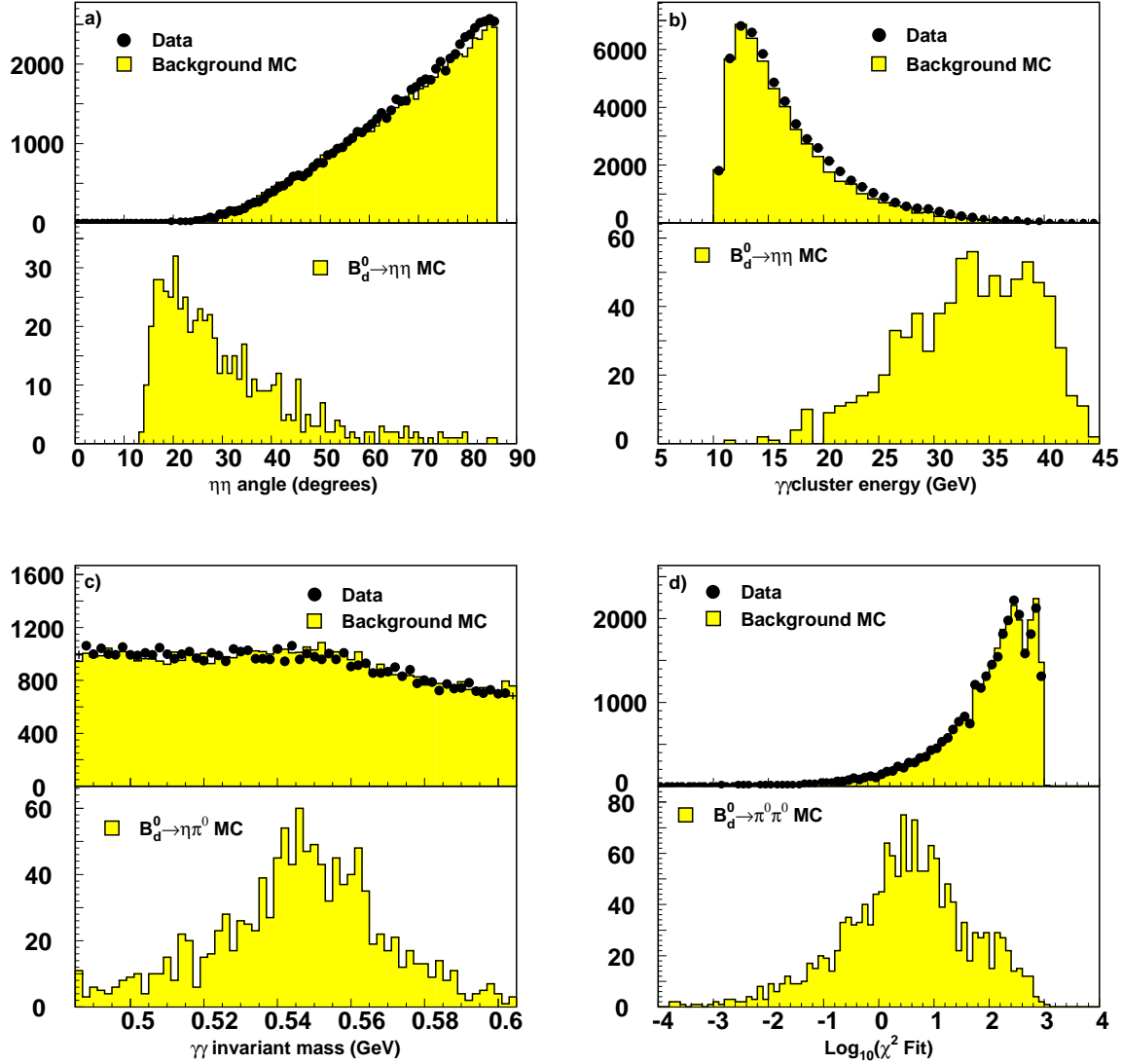


Figure 2: Some selection variables for rare B_d^0 decays for Monte Carlo of the signal, data collected in years from 1991 to 1993 and an equivalent amount of background Monte Carlo events (some preselection cuts are applied). a) Opening angle of the two reconstructed η 's of $B_d^0 \rightarrow \eta\eta$ in four detected photon final state, b) energy of the B_d^0 candidate in the $B_d^0 \rightarrow \eta\eta$ decay where one of the η 's is detected as a single cluster, c) invariant mass of the photon pair from the η candidate decay in $B_d^0 \rightarrow \eta\pi^0$, d) logarithm of the χ^2 of the constrained fit to the B_d^0 mass for the two single clusters in $B_d^0 \rightarrow \pi^0\pi^0$.

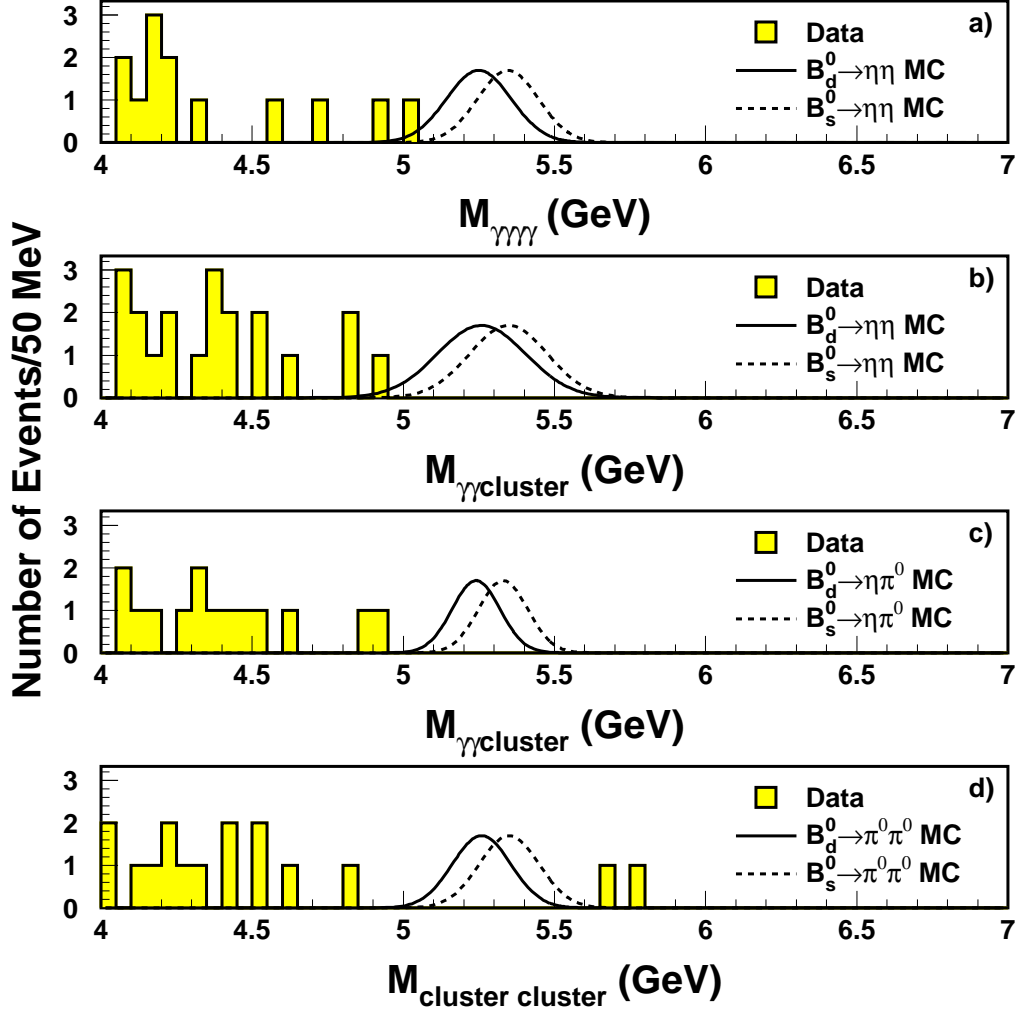


Figure 3: Invariant mass spectra for data and the expected resolutions from the $B_{d(s)}^0$ and B_s^0 Monte Carlo (arbitrary units) after the application of the final cuts. a) $B_{d(s)}^0 \rightarrow \eta\eta$ in four photons, b) $B_{d(s)}^0 \rightarrow \eta\eta$ in a photon pair plus one single cluster, c) $B_{d(s)}^0 \rightarrow \eta\pi^0$, d) $B_{d(s)}^0 \rightarrow \pi^0\pi^0$ before the application of the χ^2 cut.